Effect of Pyridazine Content and Crosslinker Structure on the Properties of Polyurethane Elastomers

Stefan Oprea

"Petru Poni" Institute of Macromolecular Chemistry, Aleea Grigore Ghica, Voda No.41-A, 700487 Iasi, Romania
Correspondence to: S. Oprea (E-mail: stefop@icmpp.ro)

ABSTRACT: This article studies the development of a series of heterocyclic polyurethanes (PUs) with various pyridazine content and different crosslinker structure in their main chains. All of the isocyanate-terminated PU prepolymers were prepared from poly(tetramethylene oxide) glycol of molecular weight 1400 (Terathane 1400) and 1,6-hexamethylene diisocyanate. The properties of the obtained linear and crosslinked pyridazine-based PU were compared with the properties of common PUs obtained by chain extension with 1,4-butanediol. All the obtained PUs were characterized through spectral and thermal behavior. The pyridazine-based PU showed improved thermal stability with 10% weight loss at temperatures above 370–400°C. With the increase of pyridazine content the values of Young's modulus are higher and the strain at break decreases. Increasing pyridazine content leads to increased films surface hydrophilicity. © 2012 Wiley Periodicals, Inc. J. Appl. Polym. Sci. 128: 3974–3981, 2013

INTRODUCTION

Polyurethanes (PUs) are widely used in industrial applications because they have excellent properties, which can be improved by changing the chemical structure of the compositions, and the microphase-separated morphologies. The PU morphology and properties can be enhanced by the introduction of new chemical structures in the backbone chains, which promote strong intermolecular association through physical crosslinks, or by chemical crosslinks that increase the structural integrity of the hard segment that results in improved properties.[1–10]

Conventional PUs exhibit poor heat resistance that limits their applicability as engineering material. The thermal stability of PUs can be improved by changing the chemical structure of the backbone chains through the introduction of thermally stable heterocyclic groups.[11–15] Unsaturated six-membered nitrogen heterocycles—such as pyridine, pyrimidine, and pyridazine—have stable aromatic rings.[16,17] Also, the heteroatom-based systems, such as pyridazine, pyridine, pyrazine, pyrine, thiophene, etc., posses a strong dipole within their structure and thus may change the polarity, regularity, and planarity of the main chain. This can lead to different thermal properties and phase transition behavior.[18,19]

Pyridazines are heterocyclic compounds with an N—N bond in their ring structure. Pyridazines are also known to exhibit biological activities such as antibacterial, antibiotic, analgesic, anti-

viral, anti-inflammatory effects, etc.[20] Thus, due to their structure, reactivity, and their tendency to form stable compounds, pyridazine derivatives have been the subject of extensive research—particularly in the pharmaceutical and agrochemical areas—because of their useful biological properties.[21,22]

In this article we obtained PUs with a heterocyclic structure in main chain and place into discussion the effect of incorporating various pyridazine content and different crosslinkers structures into the backbone chains of the PU films. The effects of the hard segments structure on the pyridazine-based PU thermal stability and mechanical properties were compared with the performance of PUs obtained with pure aliphatic diols as chain extenders. In addition, the surface properties were obtained by contact angle measurements and fluorescence spectra evaluation. The main goal is uses of the pyridazine derivative as a structural element into PU main chain.

EXPERIMENTAL

Materials

Poly(tetramethylene oxide) glycol of a molecular weight of 1400 (Terathane 1400) (Aldrich, Switzerland) was dried in high vacuum for 2 h at 120°C prior to use. All other chemicals were used as received.

3,6-Dihydroxypyridazine (DHPyd), glycerol (Gly), pyridoxine (Pyr), 2,4,6-triaminepyrimidine (TAPy), 2-amino-4,6-dihydroxypyrimidine

**Table I.** Formulations of the Obtained DHPyd-Polyurethane Elastomers

Samples	Polyether/HDI/ chain extenders molar ratio	Type of chain extenders
P0	1 :2 : 1	1,4-butane diol
P1	1 :2 : 1	3,6-dihydroxypyridazine
P2	1 :3 : 2	3,6-dihydroxypyridazine
P3	1 :4 : 3	3,6-dihydroxypyridazine
P4	1 :2 : 1	3,6-dihydroxypyridazine + glycerol
P5	1 :2 : 1	3,6-dihydroxypyridazine + pyridoxine
P6	1 :2 : 1	3,6-dihydroxypyridazine + 2,4,6-triamine-pyrimidine
P7	1 :2 : 1	3,6-dihydroxypyridazine + 2-amine-4,6-dihidroxi-pyrimidine
P8	1 : 2 : 1	3,6-dihydroxypyridazine + tiobarbituric acid

(AHPy), 2-thiobarbituric acid (TBA), and dimethylformamide (DMF) were purchased from Sigma-Aldrich and 1,6-hexamethylene diisocyanate (HDI) was obtained from Fluka (Switzerland).

Synthesis of the Polyurethane Elastomers

These PUs were prepared by the conventional two steps procedure via isocyanate-terminated prepolymer, followed by chain extension with heterocyclic diol and different crosslinkers. In the case of two different chain extenders, equal moles of the functional groups were used. The compositions of the various samples are given in Table I.

A typical two step polymerization procedure for the synthesis of these PUs is illustrated by Figure 1 and can be explained as follows. The isocyanate-terminated prepolymer was prepared by reaction of the degassed and dried Terathane 1400 (0.01 mol) and HDI (0.02 mol), in a 250 mL glass reactor equipped with a mechanical stirrer, a drying tube connected to the vacuum pump and an oil bath, at 80°C for 2 h. In the second step, the urethane prepolymer was chain-extended using the required amount of DHPyd or mixture of DHPyd and crosslinker and 20 mL DMF as the solvent at 80°C for 2 h. The PU product was then cast onto cleaned glass plates and kept at 80°C for
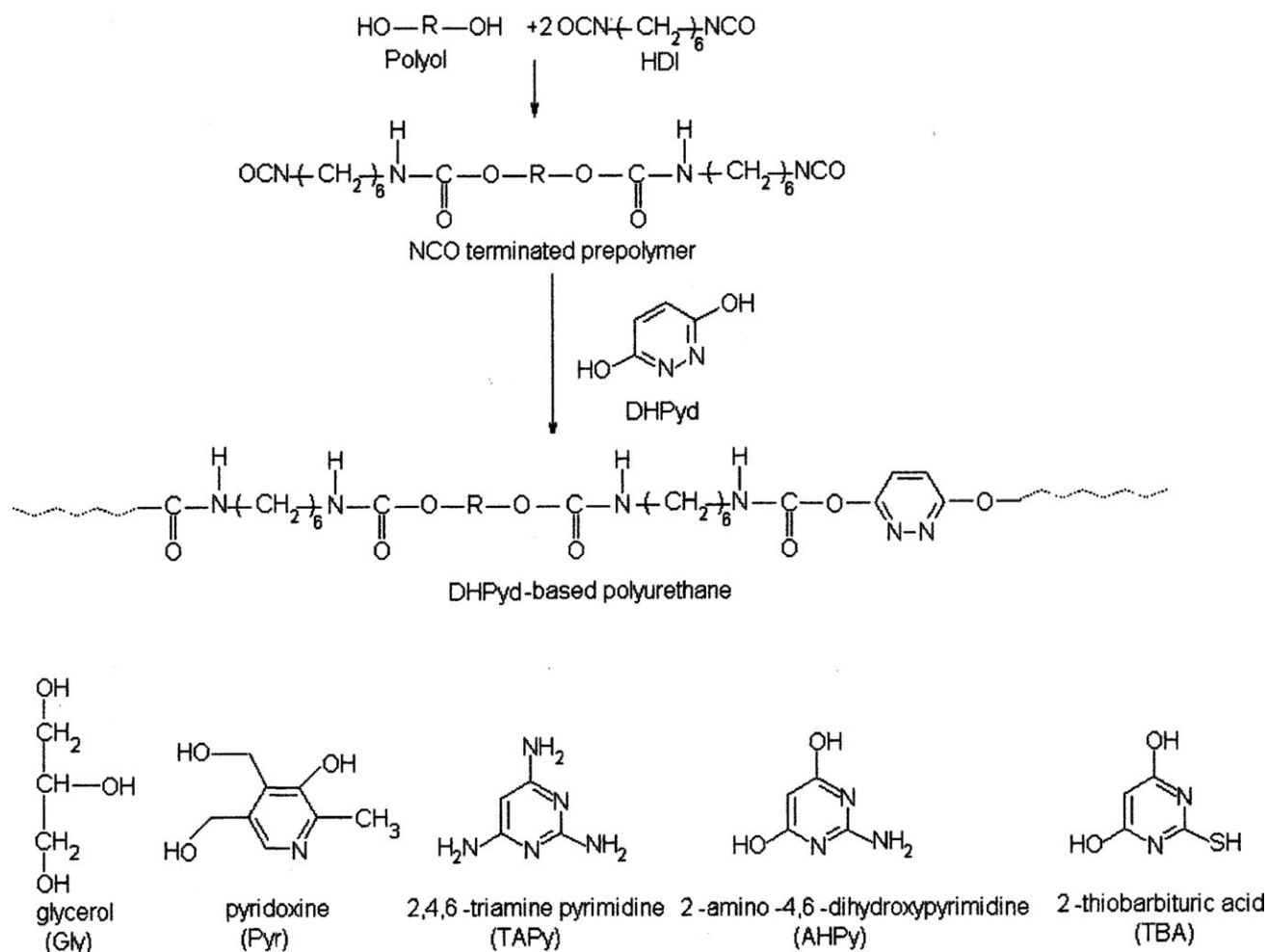
Figure 1. Schematic representation of DHPyd-based polyurethane synthesis and crosslinkers chemical structure.

24 h in order to obtain flexible PU films. PU films thus prepared were used for the determination of physico-mechanical properties and for the thermal resistance and surface behavior analysis.

Characterization

Fourier transform infrared (FTIR) spectra were recorded on a Bruker VERTEX 70 Instrument equipped with a Golden Gate single reflection ATR accessory. The spectra were recorded in the range of 600–4000 cm^{-1} with a nominal resolution of 4 cm^{-1}.

Thermogravimetric experiments took place in an air atmosphere through thermogravimetric analysis (TGA) using a DERIVATOGRAF Q-1500 D apparatus (Hungary). The rate of the TGA scans was of 10°C/min. The initial weight of the samples was ∼50 mg and the temperature range 30–700°C.

Differential scanning calorimetric (DSC) measurements of the synthesized materials were performed on a DSC-7 Perkin-Elmer at a heating rate of 20°C/min. The thermal transition behavior was studied in a temperature range of −100 to 60°C. Tests were conducted on samples of about 10 mg that were gradually heated in order to observe the glassy transition temperature (T_g). The DSC experiments were carried out with a liquid nitrogen cooler in a helium atmosphere. All DSC thermograms were taken during the first cooling cycle.

The mechanical properties were determined using a Shimadzu EZTest (Japan), equipped with a 5 kN load cell. Dumbbell-shaped specimens were prepared using dies (75 × 12.5 × 4 mm^3; ISO 37 type 2). The test specimens that were cut from the samples were no more than 0.5 mm thick. The specimens were prepared so as to be free of surface roughness, fabric layers, etc. The tests were performed at room temperature (23°C), with a cross-head speed of 50 mm/min. All the tests were conducted on five samples of each product and the averaged values were reported.

The surface tension of the PU surfaces was measured by means of static contact angle using the sessile drop method on a Dataphysics Contact Angle System KSV Instruments Ltd, Finland. Contact angle measurements were performed at room temperature using deionized water and ethylene glycol. Each contact angle measurement was recorded within the first 10–20 s following the placement of the sessile drop over a fresh surface region and the procedure was repeated for cross-verification. The contact angle was measured with an accuracy of ±2°.

Fluorescence spectra were obtained at room temperature on a LS55 PerkinElmer spectrometer (Shelton, CT, USA). The fluorescence spectra were measured at a 310 nm excitation and for emission wavelengths of 350–600 nm.

RESULTS AND DISCUSSION

The FTIR spectra were used to observe the changes in the shifts and intensity of the peaks for the N—H and C=O stretching regions in order to determine the evolution of hydrogen bonding, which is dependent on hard segment structure. The FTIR spectra of the pyridazine-based PU films are shown in Figure 2.

Linear pyridazine-based PUs present several absorption peaks at 1544, 1408, 1208, 1010, 897, 845, and 813 cm^{-1}, which are
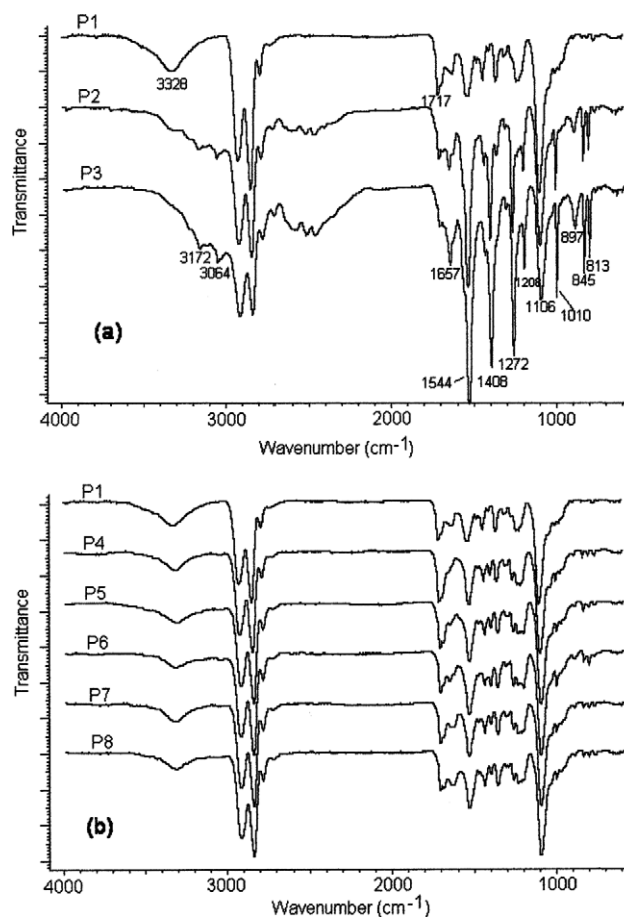
Figure 2. FTIR spectra of the (a) linear and (b) crosslinked pyridazine-based polyurethane elastomers.

characteristic for the stretching vibration of the pyridazine ring, thus proving the presence of pyridazine moieties into PU matrix. The wavelength values of the obtained peaks are close to values obtained for pure pyridazine.[23] The intensities of these characteristic pyridazine ring peaks strongly increase with an increase in DHPyd content [P1 vs. P3, Figure 2(a)]. This clearly indicates that the insertion of a pyridazine group into the PU backbone strongly improves the hydrogen bonding in the obtained PU elastomers. This is supported by the fact that the pyridazine stretching vibration bands decreased in intensity with the incorporation of crosslinkers, which hinder the hydrogen-bonding process [Figure 2(b)]. The C—O—C stretching of the PU appears as a strong peak at 1100 cm^{-1}, which proves that the ether group is also involved in H-bonding.

Also, large changes occur in the case of the —NH stretching vibration. With the increase in DHPyd content (P3), the peak from 3328 cm^{-1} disappears and new peaks appear at 3172 and 3064 cm^{-1}. These peaks correspond to the C—H aromatic stretching (CH$_s$ and CH$_{as}$). These indicate that the strength and number of urethane —NH hydrogen bonds decrease with the increase in pyridazine content. By comparison, Figure 2(b) shows that the NH stretching vibration at 3300 cm^{-1} has a similar behavior for all the crosslinked pyridazine-based PUs. This may be due to the stronger chemical crosslinking, which hinders

the free movement of the chain and achieves better packaging, and association by formation of hydrogen bonds of the pyridazine group.

The C=O region appears some changes as a function of pyridazine content or of the chemical structure of the crosslinkers (Figure 3).

The changes of the stretching vibration peaks in the range of 1717–1600 cm^{-1} shows the influence of the pyridazine moiety content on the hydrogen bonds from the PU matrix [Figure 3(a)]. Thus, the increase in DHPyd content results in a decrease of the C=O stretching from the urethane linkage from 1717 cm^{-1} and an increase of the bonded C=O stretching of the heterocyclic linkage from 1657 cm^{-1}. These two absorbing peaks can be attributed to the weakly hydrogen-bonded urethane and urea carbonyl stretching vibrations. The increased intensity of the absorbing peak at 1657 cm^{-1} shows the strength of the hard segments interaction in the pyridazine heterocyclic rings area.

The PU crosslinked with Gly (P4) exhibits a sharp peak at 1717 cm^{-1} while for the PU crosslinked with heterocyclic derivatives (P5–P8) this peak decreases in intensity [Figure 3(b)]. This can be explained by the fact that the aliphatic crosslinker (Gly) allows for a good packing of the molecular chain and the formation of a greater number of hydrogen bonds while the rigid aromatic heterocycle crosslinkers hinder the ordering of the molecular chains and the formation of hydrogen bonds. PUs obtained with crosslinkers that have —NH$_2$ in their structure show a peak at 1660 cm^{-1} that is attributed to the hydrogen-bonded urea groups (P6 and P7).

Thermal Analysis

The thermal stability of the pyridazine-based PU was investigated using TGA under air exposure. The TGA thermogram profiles of the obtained PU are shown in Figure 4.

The initial decomposition of the linear pyridazine-based PUs [Figure 4(a)] occurs at around 350°C, providing better thermal stability than common PUs chain-extended with 1,4-butanediol. In the case of pyridazine-based PUs the main weight loss (10–80%) occurred in the range of 385–475°C, in comparison with the butanediol-based PU, for which the 10–80% weight loss occurs in the range of 310–420°C. The maximum decomposition temperature of prepared polymers was observed in the range of 430–445°C. This shows that the presence of the pyridazine ring in the PU backbone chain improves thermal stability. This can be explained by the fact that pyridazine rings are more thermally-stable and thus delay urethane groups decomposition and maintain the PU matrix integrity at higher temperatures.

The crosslinked pyridazine-based PU does not achieve a significant improvement in thermal stability, except for the case of PUs with AHPy as a chain extender (P7), which exhibit a slight improvement in thermal stability [Figure 4(b)].

The slight increase in the thermal behavior of the crosslinked samples can be explained by the fact that structurally stiff matrix that was created prevented the proper packaging of the PU matrix, which would enable the formation of a sufficient number of hydrogen bonds with the pyridazine group.
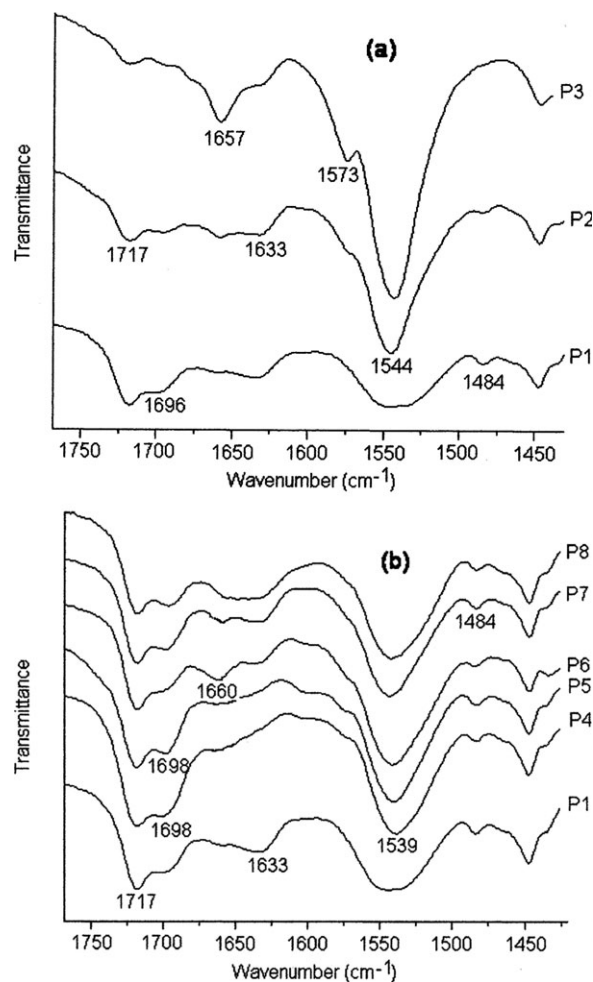

Figure 3. FTIR spectra in the 1750–1450 cm^{-1} region in (a) linear and (b) crosslinked samples.

The introduction of pyridazine rings into the PU chain increases the temperature of the 10% weight loss and with further increase in the pyridazine content the thermal stability slightly increases as well.

The DSC thermograms of pyridazine-based PU films are shown in Figure 5.

The linear pyridazine-based PUs (P1–P3) exhibited a lower soft segments glass transition in comparison with PUs chain extended with 1,4-butanediol (P0) [Figure 5(a)]. The glass transition temperature decreases from −65°C (P0) to −73°C (P3) with the increase of the DHPyd content. This is a result of the higher degree of phase separation between the hard and soft domains. Also, the aromatic nature of the heterocyclic pyridazine rings creates increased stiffness and dipole–dipole interaction that can changes the planarity of the main chains. This contributes to the decrease of the domains cohesion, as compared to the aliphatic PU chain (P0), which provides good packaging of the molecular chains.

In the case of crosslinked samples [P4–P8 from Figure 5(b)] the phase separation formation may have been inhibited by the presence of chemical crosslinks.[24] Chemical crosslinks hindered
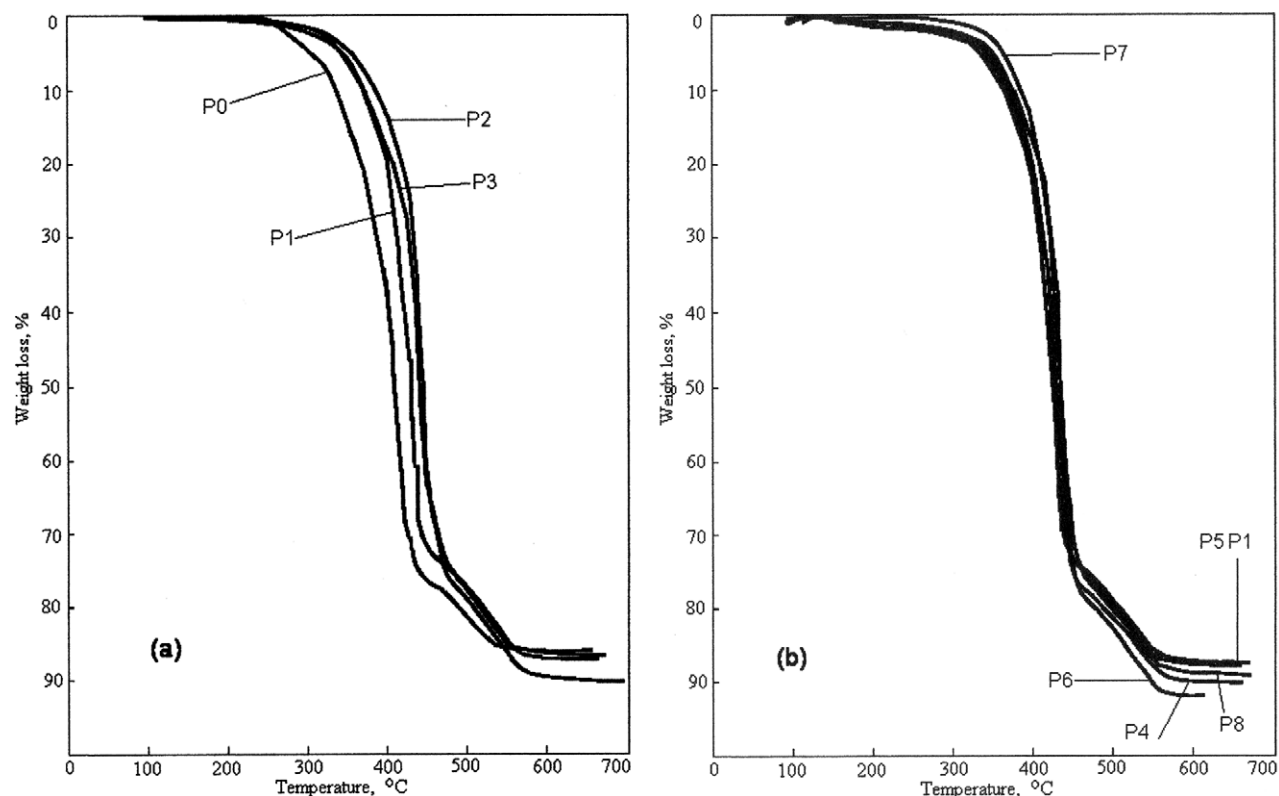
Figure 4. TGA thermograms of (a) linear and (b) crosslinked pyridazine-based polyurethanes under air atmosphere at a heating rate of 10°C/min.

the ability of the hard segments to form hydrogen bonds by reducing the mobility of the hard segments. Thus, the glass transition values are stored in the −69 and 67°C interval except for the sample crosslinked with glycerol (P4), which provided more freedom of movement and cohesion points, allowing for an increased glass transition value (−65°C).

This proves that the inter-molecular interactions, rigidity, as well as the multiaromatic heterocyclic structures of the hard segments determine thermal behavior.

Mechanical Properties

Stress–strain curves for pyridazine-based PU samples are shown in Figure 6.

These PUs exhibited a different mechanical behavior depending on the pyridazine derivative content or on the crosslinkers chemical structure. Increasing DHPyd content results in a significant increase of the initial properties (Young's modulus) from 8.6 MPa (P1) to 242 MPa (P3) as seen in Figure 6(a). In contrast, crosslinked samples (P4–P8) show a smooth transition in stress–strain behavior close to that of the sample with low content of DHPyd (P1). This shows that the chemical structure of the DHPyd chain extender increased the stiffness of the hard segment. This effect can be clearly seen when the result is compared with that of the sample chain-extended with 1,4-butanediol (P0) when submitted to identical experimental conditions. This behavior is evident in the first phase of the deformation, but stress of break shows a slight decrease with the increase in DHPyd content. Also, Figure 6(a) shows that increasing DHPyd content in the PU backbone results in a decrease of strain at break

values. Thus, strain at break decrease from 800% (P0) to 220% (P3). This can be explained by the fact that pyridazine rings change the planarity of the polymer structure, which will then strongly disturb the chain packing, compared with the linear, aliphatic butane diol chain extender. Therefore, pyridazine heterocyclic ring interrupts the chain orientation and eventually inhibits the regular chain packing of the crystallization process.[19] In general, DHPyd based-PUs exhibit good mechanical properties due to the cumulative effect of the formation quite a few of hydrogen bonds and the stiffness provided by the heterocyclic rings.

As compared with PUs with a low content of DHPyd, the stress–strain behavior of the crosslinked samples is determined by the particular structure of the crosslinker [Figure 6(b)]. It is interesting to note the behavior of the samples obtained with pyrimidine derivative as crosslinker (P6, P7, and P8), in which case the nature of the reactive groups determine the mechanical properties, and especially the percentage of elongation at break. This is a result of the weaker packing of the hard domain due to hydrogen bond loss.

Surface Properties

Contact angle analysis indicates that the pyridazine ring structure, which has a stronger polarity than a benzene ring, influences the surface hydrophilicity and surface molecular mobility of the obtained PUs. The hard segment chemical structures have a strong effect on the mobility and flexibility of the molecular chain in order to create a rich hydrophilic or hydrophobic surface.[25]
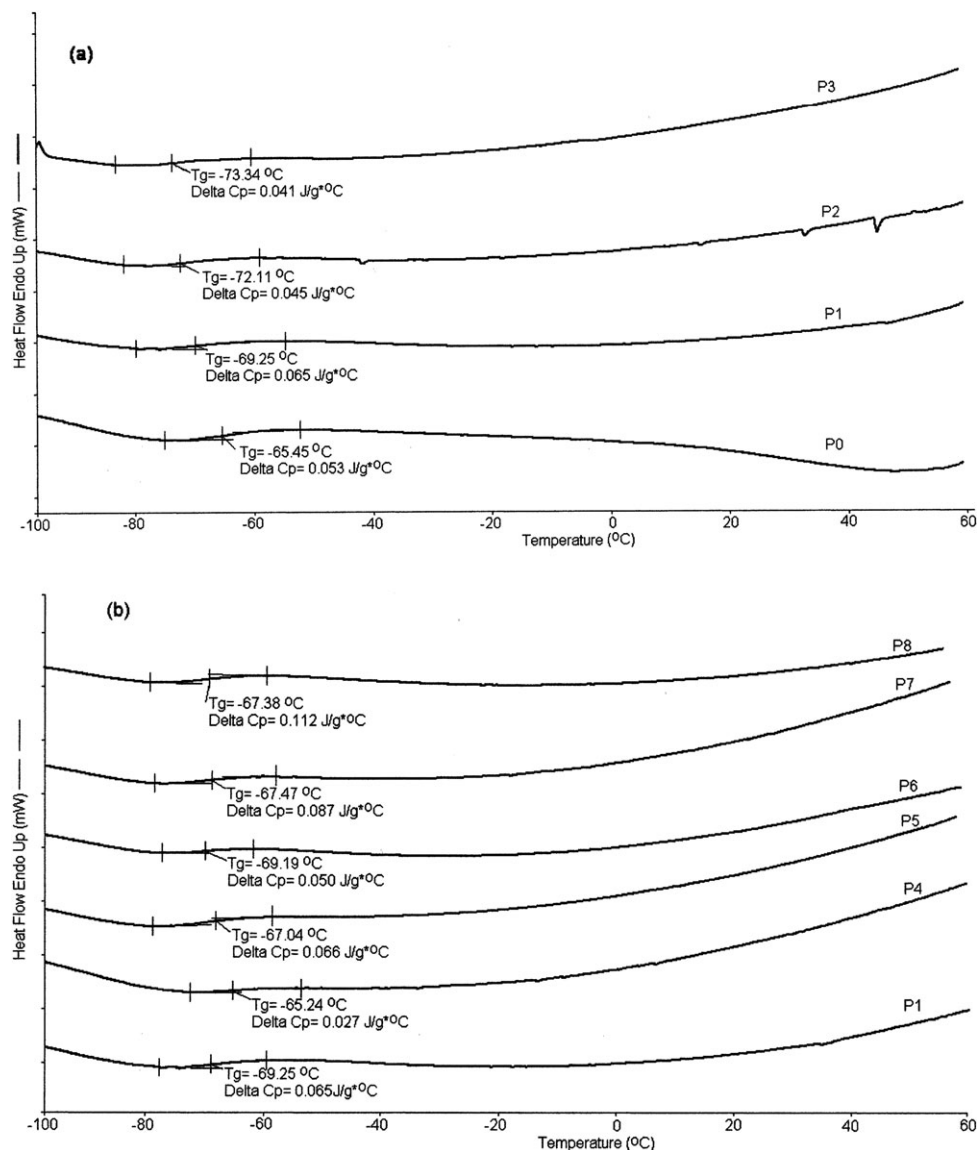
Figure 5. DSC thermograms of (a) linear and (b) crosslinked pyridazine-based polyurethane films.

The contact angle is a result of the interactions of the three interfaces as described by Young's equation[26]:

$$\gamma_{SV} = \gamma_{SL} + \gamma_{LV}\cos(\theta) \qquad (1)$$

Work of adhesion (W_a) of a liquid drop to a solid surface was calculated with Young–Dupree equation[27]

$$W_a = \gamma_{LV} + (1 + \cos\theta) \qquad (2)$$

where γ_{SV}, γ_{SL}, and γ_{LV} represent the interfacial tension of the solid/vapor, solid/liquid, and liquid/vapor interfaces. The equilibrium contact angle is represented by θ.

Table II presents the water contact angles of the linear and crosslinked pyridazine-based PU as compared with butanediol-based PU.

The values presented in the Table II show that the contact angles of water on the pyridazine-based PUs decreased as the

pyridazine content increased. Also, contact angle values are smaller than those of conventional PU obtained with butanediol. The low contact angle values of the linear PU (P1, P2, and P3) are due to the multiple pyridazine rings from the hard segments, which possess a strong dipole within their structure and thus change the planarity of the molecular chain so that hydrogen bonds do not hinder polar groups from migrating towards the PU film surface.

Crosslinked samples exhibit contact angle values that vary as a function of crosslinker structure. Thus the lowest (86°) was obtained for PUs crosslinked with glycerol (P4), because of its hydrophilic nature and elasticity that facilitate the migration of the polar group to the film surface. The highest (98°) was obtained for PU crosslinked with TAPy (P6). This result is caused by the multiple hydrogen bonds between the NH of the urea groups and urethane or urea carbonyl groups, bonds which firmly prevented the polar groups from getting close to the material surface.
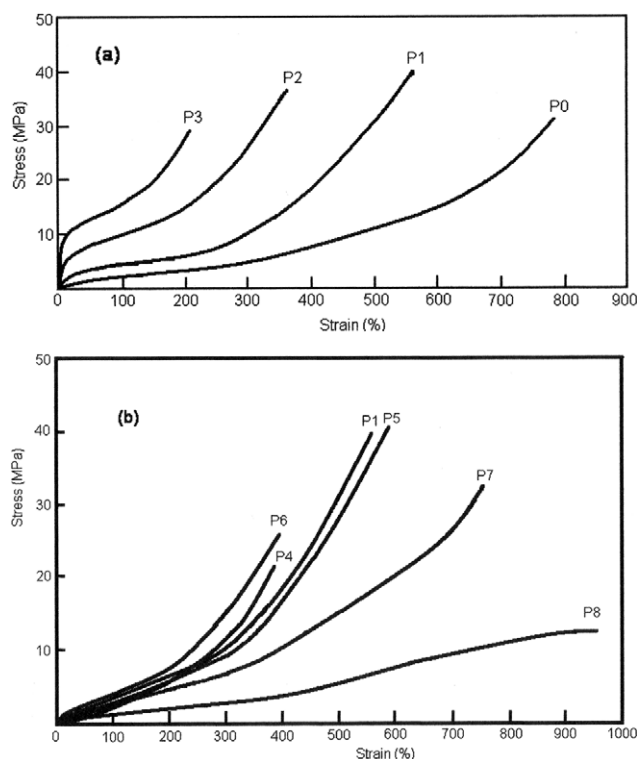
Figure 6. Stress versus strain curves for (a) linear and (b) crosslinked pyridazine-based polyurethane films.

As can be seen from Table II, the contact angle of ethylene glycol with the pyridazine-based PU films follows the same trend as water but with smaller variations. Water and ethylene glycol were used because they have highly similar cohesive energy densities. Also, making measurements of contact angles using two different liquids helps better calculate the surface energy parameters.

The surface free energy is deduced from Young's equation considering that the total surface tension γ is given by γ^d-representing the dispersive contribution to the surface tension, and γ^p-being the polar component of the surface tension so that:

Table II. Contact Angle (θ) and Work of Adhesion (W_a) Values of the Pyridazine-Based Polyurethane Films Surfaces

|	Water		Ethylene glycol	
Sample	θ (°)	W_a (mN/m)	θ (°)	W_a (mN/m)
P0	101	58	72	63
P1	93	68	71	63
P2	87	76	67	67
P3	81	83	61	70
P4	86	78	62	70
P5	88	75	63	70
P6	98	62	74	61
P7	89	74	65	68
P8	93	68	66	67

Table III. Interfacial Tension for a Solid–Liquid System (γ_{sl}) in Pyridazine-Based Polyurethane Films

			γ_{sl} (mN/m)	
Sample	λ_{sv}^{p} (mN/m)	λ_{sv}^{d} (mN/m)	Water	Ethylene glycol
P0	0.3	29.5	44.3	14.6
P1	4.3	17.6	25.9	6.6
P2	7.4	16.2	20.0	4.5
P3	10.9	15.1	15.3	3.3
P4	6.4	20.1	21.3	4.2
P5	4.9	22.2	24.3	5.1
P6	1.9	20.5	33.3	9.7
P7	5.3	19.6	23.5	5.2
P8	2.3	24.9	31.6	8.1

p, polar; d, disperse.

$$\gamma = \gamma^d + \gamma^p$$

The values of the surface tension decrease with the increase in DHPyd content (Table III).
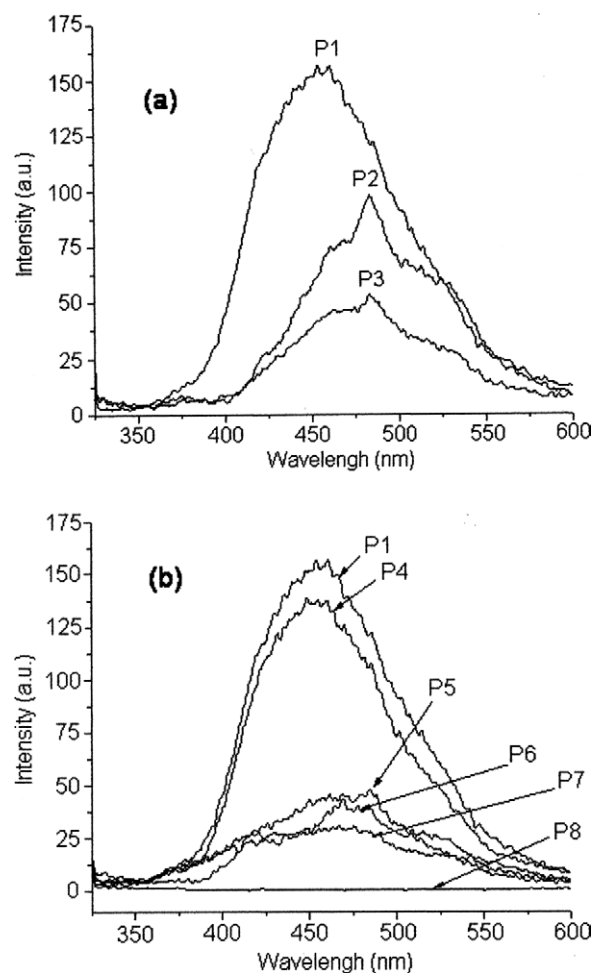
Figure 7. Emission spectra (excitation at 310 nm) of (a) linear and (b) crosslinked pyridazine-based polyurethane films.

Variations in contact angle and surface tension can be the result of the different chemical composition of the hard segments but also of the various morphologies of the surface structure.[26] PUs with different crosslinker structure will present different surface mobility and surface tension.

The fluorescence spectra of the DHPyd-based PU, determined at an excitation wavelength of 310 nm, are shown in Figure 7.

The linear DHPyd-based PU elastomers (P1, P2, and P3) exhibit a high intensity emission peak, which shifts with the increase in pyridazine content from 454 (P1) to 483 nm (P2 and P3). Nonetheless, the intensity of this peak decreases with the increase of pyridazine content. For crosslinked samples the emission peaks shifted to higher wavelength values and decreased in intensity as a function of the rigidity of the resulted structure and chemical crosslinks. Thus, in case of samples crosslinked with glycerol (P4), the emission fluorescence peaks remain at wavelengths values and intensity similar to those of PU obtained with low pyridazine content (P1). This is due to the freedom of movement of the molecular chain provided of glycerol.

CONCLUSIONS

A series of linear and crosslinked PUs were obtained using different content of pyridazine–diol as chain extender. The different crosslinker chemical structure was used to influence the hard segment structure, which was then studied in order to determine the effects of this change on the PU properties. The properties of PUs with a pyridazine heteroatom ring in the main chain were compared with those of common PUs chain-extended with butane diol.

The presence of pyridazine derivatives in the main chain affects molecular chain planarity, which results in a slight decrease of the mechanical properties as compared to those of conventional PU. The introduction of pyridazine derivatives in the main chain clearly enhances the thermal stability of the obtained PU films as compared to the properties exhibited by PUs chain-extended with butane diol. Also, the contact angle and surface energy decrease significantly with increasing the amount of pyridazine moiety into the PU matrix, as the PUs become hydrophilic.

REFERENCES

1. Mallakpour, S.; Tirgir, F.; Sabzalian M. R. *J. Polym. Environ.* **2010**, *18*, 685.

2. Biemond, G. J. E.; Gaymans, R. J. *J. Mater. Sci.* **2010**, *45*, 158.

3. Lee, H. T.; Lin, L. H. *Macromolecules* **2006**, *39*, 6133.

4. Varkey, E. C.; Sreekumar, K. *J. Mater. Sci.* **2010**, *45*, 1912.

5. Oprea, S. *J. Mater. Sci.* **2011**, *46*, 2251.

6. Kuriyagawa, M.; Kawamura, T.; Hayashi, S.; Nitta, K. *J. Mater. Sci.* **2011**, *46*, 1264.

7. Oprea, S. *J. Am. Oil Chem. Soc.* **2010**, *87*, 313.

8. Liao, L.; Cao, Q.; Liao, H. *J. Mater. Sci.* **2010**, *45*, 2436.

9. Azzam, R. A.; Mohamed, S. K.; Tol, R.; Everaert, V.; Reynaers, H.; Goderis, B. *Polym. Degrad. Stab.* **2007**, *92*, 1316.

10. Yeganeh, H.; Talemi, P. H.; Jamshidi, S. *J. Appl. Polym. Sci.* **2007**, *103*, 1776.

11. Liu, J.; Ma, D.; Li, Z. *Eur. Polym. J.* **2002**, *38*, 661.

12. Oprea, S. *High Perform. Polym.* **2012**, *24*, 389.

13. Chen, X.-D.; Zhou, N.-Q.; Zhang, H. *J. Biomed. Sci. Eng.* **2009**, *2*, 245.

14. Oprea, S. *Polym. Bull.* **2010**, *65*, 753.

15. Flores, M.; Fernández-Francos, X.; Morancho, J. M.; Serra, A.; Ramis, X. *J. Appl. Polym. Sci.* **2012**, *125*, 2779.

16. Oprea, S.; Potolinca, V. O. *Design. Monom. Polym.* **2010**, *13*, 523.

17. Oprea, S.; Potolinca, V. O. *J. Mater. Sci.* **2012**, *47*, 677.

18. Demus, D.; Goodby, J.; Gray, G. W.; Spiess, H.-W.; Vill, V. Handbook of Liquid Crystals, Vol. 1: Fundamentals; Wiley-VCH: Weinheim, **1998**, pp 136–137.

19. Teoh, M. M.; Liu, S. L.; Chung, T. S. *J. Polym. Sci. Part B: Polym. Phys.* **2005**, *43*, 2230.

20. Lin, S.; Liu, Z.; Hu, Y. *J. Comb. Chem.* **2007**, *9*, 742.

21. Kandile, N. G.; Mohamed, M. I.; Zaky, H.; Mohamed, H. M. *Eur. J. Med. Chem.* **2009**, *44*, 1989.

22. Wisian-Neilson, P.; Allcock, H. R.; Wynne, K. J. Inorganic and Organometallic Polymers II: Advanced materials and Intermediates; ACS Symposium Series 572; Division of Polymer Chemistry: Denver, CO, **1994**; pp 442–497.

23. Breda, S.; Reva, I. D.; Lapinski, L.; Nowak, M. J.; Fausto, R. *J. Mol. Struct.* **2006**, *786*, 193.

24. Chattopadhyay, D. K.; Raju, K. V. S. N. *Prog. Polym. Sci.* **2007**, *32*, 352.

25. Wu, J.; Ge, Q.; Mather, P. T. *Macromolecules* **2010**, *43*, 7637.

26. Alves, P.; Coelho, J. F. J.; Haack, J.; Rota, A.; Bruinink, A.; Gil, M. H. *Eur. Polym. J.* **2009**, *45*,1412.

27. Schrader, M. E. *Langmuir* **1995**, *11*, 3585.